was expressed in podocytes in NEP25/LMB2 mice on *day 1* by serial section analysis, and it was absent in control mice (Fig. 2*H*). Electron microscopy showed the association of endothelial injury and overlaying podocyte damage in NEP25/LMB2 mice (Fig. 2*I*).

Inhibition of PAI-1 Ameliorated Microangiopathy and Protected Podocyte Loss

Treatment with the PAI-1 inhibitor TM5484 decreased glomerular PAI-1 expression in NEP25/LMB2 mice on *day 1* compared with vehicle-treated mice (Fig. 3*A*). TM5484 significantly ameliorated proteinuria and thrombosis and preserved podocyte numbers compared with NEP25/LMB2 + VH mice (Fig. 3, *B–D*). In addition, glomerular mRNA levels of eNOS and VEGF in NEP25/LMB2 + PI mice were higher and podocyte injury markers desmin and vimentin were lower than those in NEP25/LMB2 + VH mice (Fig. 3*E*). Light and electron microscopy showed that glomerular structure and podocytes were preserved and glomerulosclerosis was significantly decreased in NEP25/LMB2 + PI mice on *day 12* (Fig. 4, *A* and *B*). Immunofluorescence microscopy revealed that β_1-integrin on the basal surface of podocytes did not colocalize with synaptopodin in control or NEP25/LMB2 + PI mice, whereas β_1-integrin was located in the cytoplasm of podocytes in NEP25/LMB2 + VH mice, indicating that PAI-1-mediated β_1-integrin translocation in NEP25/LMB2 mice was protected by PAI-1 inhibitor in vivo (Fig. 5).

Heparin Loading Interfered With Thrombi But Had No Effect on Podocyte Protection

Heparin loading experiments showed no effect on proteinuria and podocyte number despite the suppression of throm-

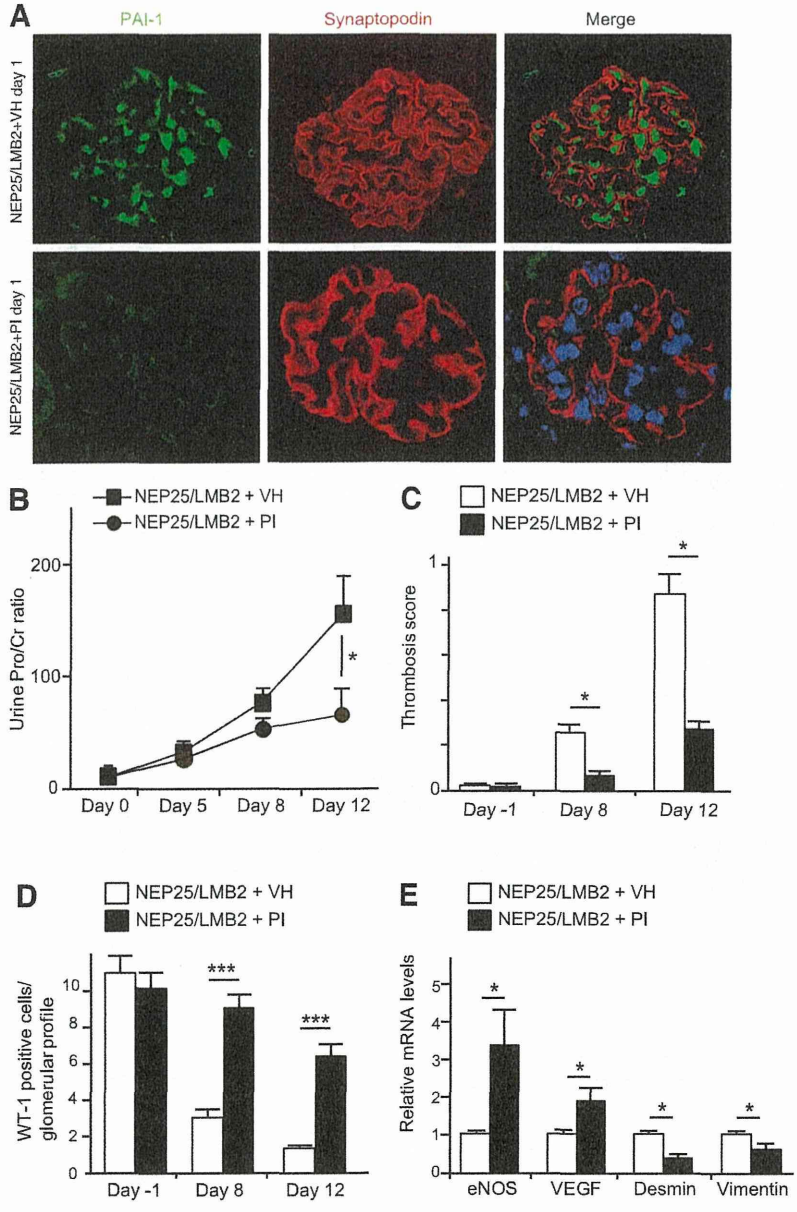

Fig. 3. PAI-1 inhibitor ameliorated proteinuria and preserved podocyte numbers in NEP25/LMB2 mice. *A*: expression of PAI-1 was reduced in PAI-1 inhibitor-treated NEP25/LMB2 mice (NEP25/LMB2 + PI group) compared with vehicle-treated NEP25/LMB2 mice (NEP25/LMB2 + VH group). *B*: proteinuria in NEP25/LMB2 + PI mice (n = 8) was significantly lower than that in NEP25/LMB2 + VH mice (n = 6) on *day 12*. *$P < 0.05$. *C*: the thrombosis score was significantly lower in NEP25/LMB2 + PI mice (n = 8) than in NEP25/LMB2 + VH mice (n = 6). *$P < 0.05$. *D*: mean WT-1-positive cells per glomerular profile in NEP25/LMB2 + PI mice (n = 8) were significantly higher than those in NEP25/LMB2 + VH mice (n = 6). ***$P < 0.001$. *E*: relative mRNA expression from isolated glomeruli on *day 12* in NEP25/LMB2 + PI mice (n = 5) and NEP25/LMB2 + VH mice (n = 5) was compared. Glomeruli were isolated from each mouse, and quantitative real-time PCR was done on each sample. NEP25/LMB2 + PI mice showed significantly higher levels in eNOS and VEGF mRNA but significantly lower levels of desmin and vimentin mRNA compared with NEP25/LMB2 + VH mice.

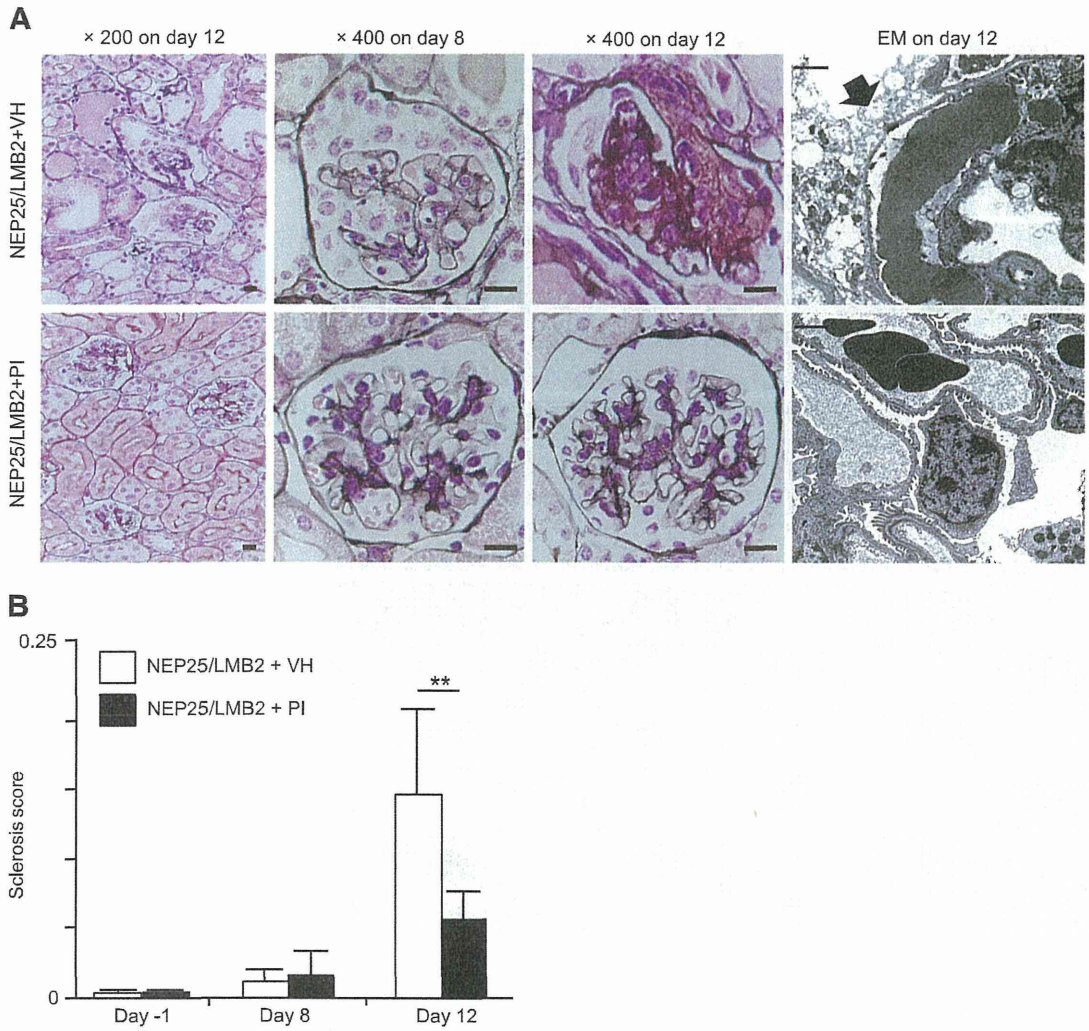

Fig. 4. PAI-1 inhibitor protected glomerular structure and podocyte injury in NEP25/LMB2 mice. *A*: histology of the kidney cortex. At lower magnification (×200; scale bars = 15 μm), NEP25/LMB2 + PI mice showed less glomerular injury and tubular dilatation than NEP25/LMB2 + VH mice (*left*). Higher magnification (×400, scale bars = 15 μm) of periodic acid-silver methenamine staining revealed glomerular epithelial proliferation and thrombi on *day 8* (*middle left*) and glomerulosclerosis on *day 12* (*middle right*) in NEP25/LMB2 + VH mice. Bowman's space cells were interpreted as proliferating parietal epithelial cells and may well represent podocytes undergoing detachment in NEP25/LMB2 + VH mice on *day 8*. Relatively normal glomeruli were noted in NEP25/LMB2 + PI mice. A transmission EM image of the glomerulus on *day 12* is shown on the *right*. In NEP25/LMB2 + VH mice, thrombotic formation was associated with degeneration in overlaying podocytes (arrow). These features were not observed, and the foot process was preserved in NEP25/LMB2 + PI mice. Scale bars = 2 μm. *B*: prevalence of glomerulosclerosis in NEP25/LMB2 mice with or without PAI-1 inhibitor. The sclerosis score was significantly lower in NEP25/LMB2 + PI mice (n = 8) than in NEP25/LMB2 + VH mice (n = 6). $^{**}P < 0.01$.

botic formation, suggesting that thrombi per se do not act on podocyte loss (Fig. 6, *A–C*).

PAI-1/uPA Complex-Induced Podocyte Detachment In Vitro Required uPAR-Dependent β_1-Integrin Endocytosis

The mechanism underlying podocyte protection by the PAI-1 inhibitor in vivo was tested using established mouse podocytes in vitro. PAI-1/uPA-treated podocytes showed a significant cell detachment with a loss of arborized shape, whereas this was not seen in podocytes treated with uPA and PAI-1 alone. Apoptotic bodies and caspase-3-positive cells were not observed upon podocyte detachment (data not shown). In addition, podocytes treated with anti-uPAR antibody targeting the PAI-1/uPA complex (anti-uPAR + PAI-1/uPA) did not exhibit podocyte detachment, indicating that PAI-1/uPA-mediated podocyte detachment was uPAR dependent (Fig. 7). Using confocal immunofluorescence microscopy, cultured podocytes treated with the PAI-1/uPA complex expressed β_1-integrin in the cytoplasm that colocalized with uPAR expression, despite the absence of such translocation in podocytes treated with uPA or PAI-1 alone or with anti-uPAR + PAI-1/uPA (Fig. 8, *A* and *B*). Biotinylated experiments showed a reduction of membrane β_1-integrin only in PAI-1/uPA-treated cells. Western blot analysis showed an increase of β_1-integrin in the cytoplasmic fraction of PAI-1/uPA-treated podocytes but not those with other treatments (Fig. 9, *A* and *B*). In addition, double immunogold labeling electron microscopy showed a disappearance of cell surface

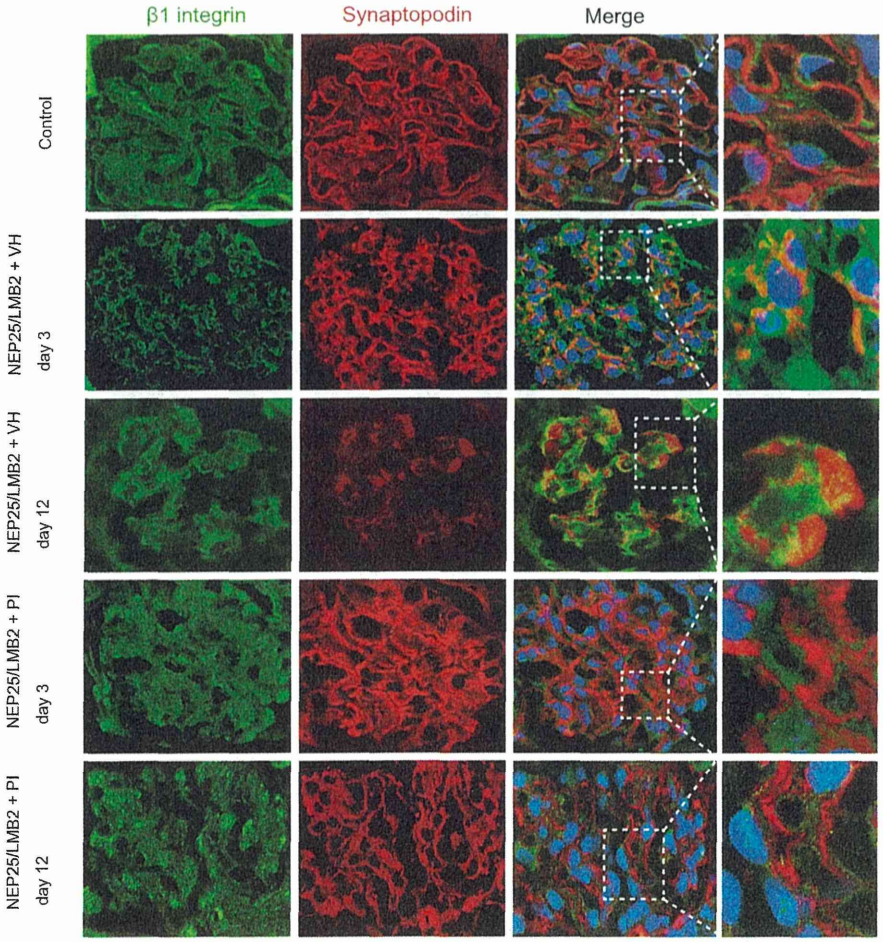

Fig. 5. β_1-Integrin was expressed in the cytoplasm of podocytes in NEP25/LMB2 mice. In control mice, β_1-integrin was detected in the mesangium and along the glomerular basement membrane (GBM) and did not overlap with synaptopodin. In NEP25/LMB2 + VH mice on *days 3* and *12*, β_1-integrin was found in the podocyte cytoplasm and occasionally colocalized with synaptopodin. Such β_1-integrin translocation was not apparent in NEP25/LMB2 + PI mice on *days 3* and *12*. Magnification: ×600.

β_1-integrin and colocalization of β_1-integrin and uPAR within the endocytotic vesicles of PAI-1/uPA-treated podocytes (Fig. 9*C*). The cytoplasmic shift of β_1-integrin and uPAR was confirmed by counting gold particles (Fig. 9*D*).

DISCUSSION

The present study describes novel mechanism of podocyte loss by aberrant intracapillary signaling, which, in turn, targets podocytes by pathological PAI-1-mediated and uPAR-dependent β_1-integrin internalization, resulting cell detachment.

Our first observation was that induced podocyte-specific injury correlated with thrombosis in glomeruli. Double immunolabeling and electron microscopy displayed an association of focal thrombi with damage in overlying podocytes. Because our heparin loading experiments suppressed thrombi without changing podocyte number, thrombosis has no significant responsibility for podocyte loss. These findings support the notion that podocyte dysfunction causes glomerular TMA and suggests that podocyte-intracapillary signaling is locally regulated. Generally, TMA appeared in the setting of severe endothelial cell injury, such as hemolytic uremic syndrome, which seems to be mediated by PAI-1, a strong effector of antifibrinolysis (2, 31). Normally, PAI-1 is not produced in kidneys but is elevated in glomeruli in cases with crescentic glomerulonephritis, which accompanies fibrin exudation (20). This may reflect severe glomerular endothelial cell injury and is thought to be a response to tissue fibrinolysis.

In our model of NEP25/LMB2 mice, expression of glomerular PAI-1 protein revealed some unique features, i.e., a diffuse pattern in a de novo fashion in glomerular endothelial cells as early as 1 day after LMB2 injection. Since LMB2 binds to human CD25 and mouse endothelial cells do not express it, glomerular PAI-1 upregulation 1 day after LMB2 injection is caused by LMB2-induced podocyte injury but not a direct action of LMB2 in glomerular endothelial cells (26).

Notably, this was before decreases in VEGF and eNOS mRNA expression as well as the formation of glomerular TMA lesions. The ultrastructure on *day 1* showed podocyte foot process effacement accompanied by endothelial cell swelling but not with platelet accumulation or thrombi in NEP25/LMB2 mice. Because LMB2 immediately binds to and injures podocytes, diffuse PAI-1 expression in endothelial cells on *day 1* suggests that PAI-1 synthesis is an early endothelial response to podocyte injury but may not be the same for antifibrinolytic actions. Of note, we also demonstrated de novo expression of uPAR in podocytes, not in endothelial cells, on *day 1*. Thus, podocyte injury rapidly activates aberrant endothelium-podocyte signaling in vivo. At the later stage where glomerular TMA was apparent, PAI-1 was also expressed in preserved capillaries but not in the portion of thrombi, implicating that

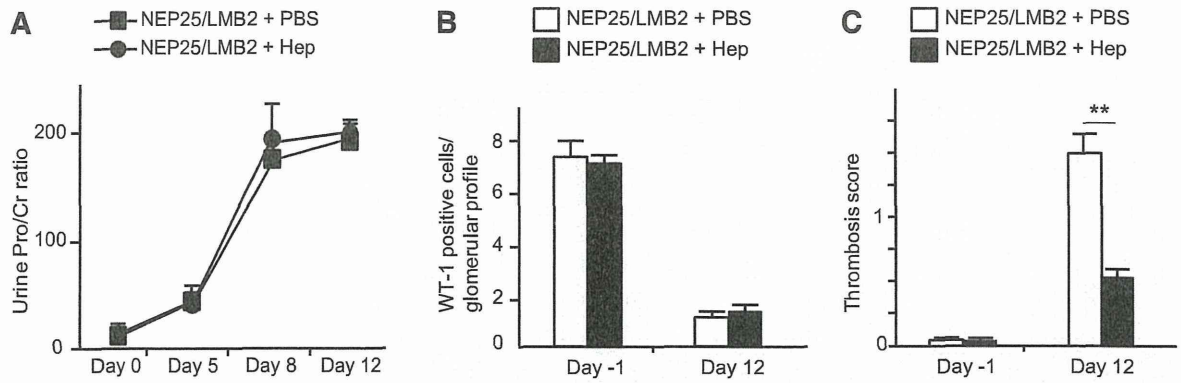

Fig. 6. Interference with thrombosis by heparin loading had no effect on proteinuria and podocyte numbers. *A*: proteinuria levels were similar in mice treated with (NEP25/LMB2 + Hep group; $n = 5$) or without heparin (NEP25/LMB2 + PBS group; $n = 5$). *B*: mean WT-1-positive cells per glomerular profile in NEP25/LMB2 + Hep mice ($n = 5$) were similar to those in NEP25/LMB2 + PBS mice ($n = 5$) on *days −1* and *12*. *C*: the thrombosis score in NEP25/LMB2 + Hep mice ($n = 5$) was significantly lower on *day 12* compared with that in NEP25/LMB2 + PBS mice ($n = 5$). $^{**}P < 0.01$.

activated endothelial cells persistently expressed PAI-1. The absence of PAI-1 at thrombi may be due to the loss of endothelial cells, as shown in our electron microscopy experiments (Fig. 1*G*). Importantly, we showed colocalization of PAI-1and synaptopodin in this late stage. Since uPAR, a receptor of PAI-1, was shown to be expressed in podocytes among several models of nephrosis (41), endothelium-derived PAI-1 may pass through the GBM and form a complex with uPAR during podocyte injury.

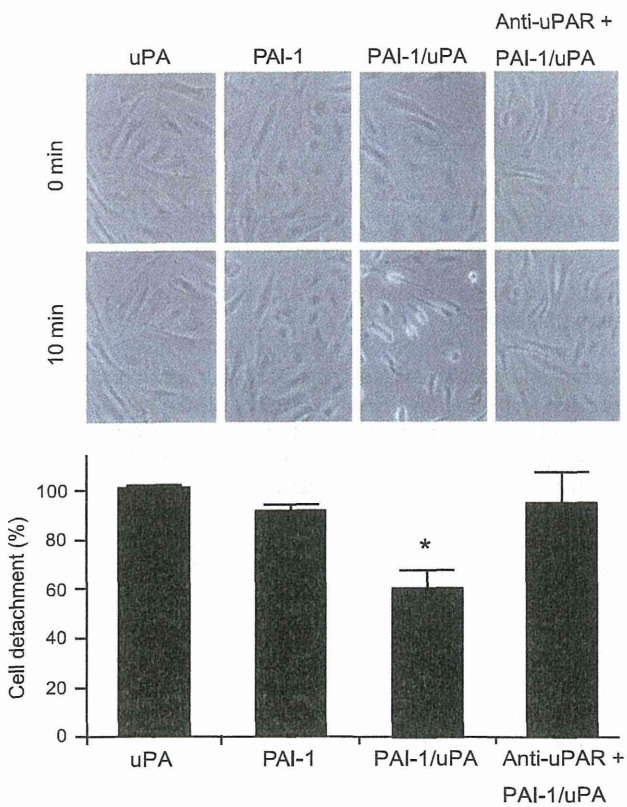

Fig. 7. PAI-1 and the uPA complex induced cell detachment in podocytes in vitro. We evaluated podocyte adhesive capabilities by manual counting cells. All experiments were repeated three times and statistically estimated. The number of podocytes incubated with the PAI-1/uPA complex was significantly reduced compared with those incubated with uPA, PAI-1 alone, and anti-uPAR + PAI-1/uPA. $^{*}P < 0.05$ vs. uPA, PAI-1, and anti-uPAR + PAI-1/uPA.

PAI-1 is known to have pleiotropic functions, including effects on cell motility, activation of apoptosis, and promotion of cell senescence, some of which may contribute to the progression of glomerular damage (9, 11, 24, 35). Although several reports have shown glomerular PAI-1 expression in glomerular diseases (14, 29, 45), the role of PAI-1 in podocyte diseases has not been extensively explored. In this regard, the present study investigated the actions of PAI-1 during podocyte injury by several experiments. First, we administered a PAI-1 inhibitor immediately after LMB2 treatment and found suppression of thrombosis and maintained VEGF and eNOS levels in NEP25/LMB2 mice, suggestive of endothelial protection. Moreover, PAI-1 inhibitor treatment showed significantly less proteinuria and higher podocyte numbers in NEP25/LMB2 mice compared with vehicle-treated NEP25/LMB2 mice. This suggests that intracapillary PAI-1 impacted the glomerular filtration barrier and particularly promoted podocyte loss. Second, because it is unknown whether the effect of PAI-1 inhibitor on podocyte protection was by direct or indirect actions through fibrinolysis, we performed heparin loading experiments in our model. Heparin loading significantly reduced thrombosis but had no effects on proteinuria and podocyte number. These observations may provide a novel action of PAI-1, other than fibrinolysis, as an aberrant intracapillary podocyte danger signal during podocyte injury.

Our hypothesis that primary podocyte injury causes secondary podocyte loss by the above-described PAI-1 mechanism suggests a positive feedback loop of podocyte loss. Using podocyte-specific CD25 chimeric mice, Matsusaka et al. (25) showed that LMB2 induced primary podocyte injury in CD25-positive podocytes only, even though neighboring podocytes lacking CD25 were secondarily damaged. This observation provides important clues to understanding progressive glomerulosclerosis promoted by a vicious cycle of podocyte loss as a "domino effect," and our hypothesis of an intracapillary danger signal toward podocytes may explain this phenomenon.

Our additional experiments in vitro disclosed the mechanism whereby intracapillary PAI-1 upregulation triggered secondary to podocyte loss. Basically, motility of cells requires the proper function of cytoskeletal and cell membrane dynamics (4). It is

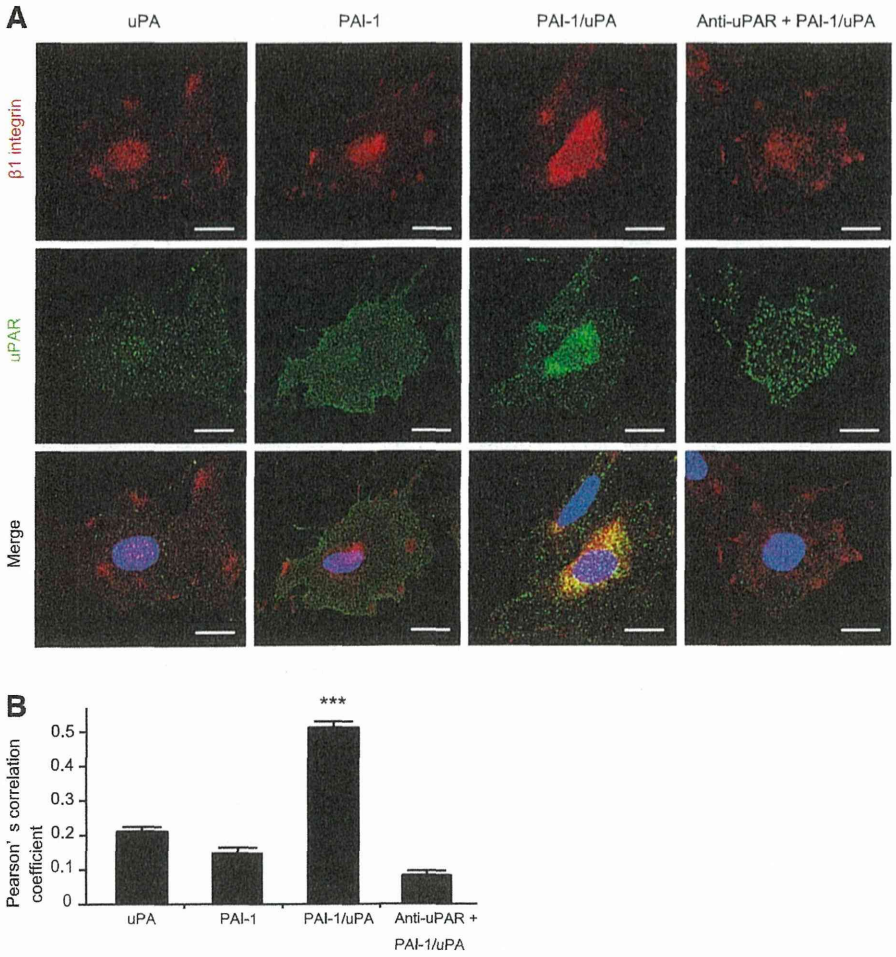

Fig. 8. The PAI-1/uPA complex induced translocation of β_1-integrin from the podocyte surface to the cytoplasm via a uPAR-dependent mechanism. *A*: localization of β_1-integrin and uPAR was visualized by confocal laser scanning microscopy. Using immunofluorescence microcopy, cultured podocytes treated with the PAI-1/uPA complex expressed β_1-integrin in the cytoplasm that colocalized with uPAR, whereas no translocalization occurred in podocytes treated with uPA or PAI-1 alone. β_1-Integrin translocalization in response to PAI-1/uPA could be inhibited by the administration of anti-uPAR. Magnification: ×1,000. Scale bars = 10 μm. *B*: colocalization between β_1-integrin and uPAR was significantly augmented in PAI-1/uPA-treated cells (n = 30 cells/group). ***P < 0.001 vs. uPA, PAI-1, and anti-uPAR + PAI-1/uPA. Pearson's correlation coefficient for β_1-integrin and uPAR colocalization was calculated using ImageJ and JaCoP software (3, 34). In every experiment using JaCoP software, the red fluorescence indirectly emitted by β_1-integrin was primarily detected in Ch1 and the green fluorescence indirectly emitted by uPAR was primarily detected in Ch2. In all calculations, the background was subtracted from the intensity values.

known that tissue PAI-1 acts to promote cell motility and proliferation by the uPA/uPAR complex, one of the mechanisms of cancer metastasis (5, 6, 37). Integrins are key molecules maintaining cell integrity via matrix-cytoskeleton signaling as transmembrane receptors (4).

In the podocyte, $\alpha_3\beta_1$-integrin is the main contributor of tight adhesion of podocytes to the GBM (32). Podocyte-specific β_1-integrin$^{flox/flox}$ mice exhibit foot process effacement, podocyte loss, and glomerulosclerosis (30). Czekay et al. (5, 6) showed that PAI-1/uPA complex-bound uPAR on the cell membrane promoted endocytosis of $\alpha_v\beta_3$-, $\alpha_v\beta_5$-, and $\alpha_3\beta_1$-integrins. In the present study, NEP25/LMB2 mice showed β_1-integrin in the podocyte cytoplasm on *day 12*, which was not observed in control mice, and was blocked by PAI-1 inhibitor. Additionally, immortalized podocytes treated with the PAI-1/uPA complex underwent significant cell detachment. Confocal immunofluorescence microscopy showed β_1-integrin and uPAR internalization only in PAI-1/uPA-treated podocytes. PAI-1/uPAR-mediated β_1-integrin internalization was confirmed by decreased membrane-localized β_1-integrin by biotinylated experiments and an increase of β_1-integrin protein in the cytoplasmic fraction. Furthermore, the double immunogold labeling technique displayed colocalization of β_1-integrin and uPAR within endocytotic vesicles after PAI-1/uPA treatment, suggesting endocytosis as a mechanism of β_1-integrin internalization.

In patients with FSGS, soluble uPAR is elevated in the serum and on the surface of podocytes. Wei et al. (41, 42) recently reported that uPAR-activated podocyte $\alpha_v\beta_3$-integrin resulted in the effacement of foot processes through disruption of the actin cytoskeleton. This mechanism could prime podocyte for detachment and then could be followed by endothelial PAI-1 induction, setting a progressive mechanism into motion. Clearly, more experiments are needed to link (soluble) uPAR-mediated podocyte injury and PAI-1-uPAR-β_1-integrin internalization, even though it is known that repression of β_1-integrin activates β_3-integrin via Rac1 and ERK (15). These observations, together with our present findings, suggest that primary podocyte injury accelerates progressive podocyte loss by upregulation of endothelial PAI-1-mediated podocyte β_1-integrin endocytosis. uPAR may have an important role in orchestrating disruption of integrin homeostatic functions to accelerate the cascade of responses leading to podocyte loss. The present study not only describes a novel mechanism of podocyte loss but also suggests that the PAI-1 inhibitor may be a possible therapeutic option for podocyte protection through the stabilization of β_1-integrin, similar to the suggested role for the B7-1 inhibitor abatacept (46). These

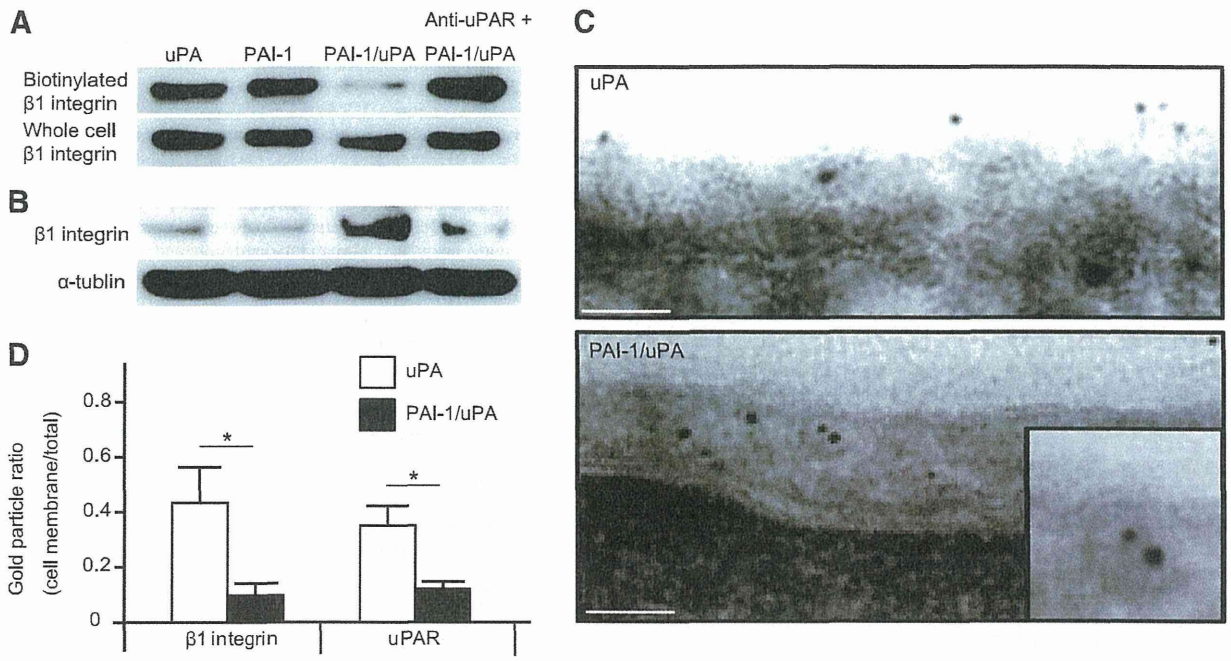

Fig. 9. The PAI-1/uPA complex induced β_1-integrin and uPAR translocation via an endosomal pathway. *A*: biotinylated experiments with Western blot analysis of β_1-integrin expression revealed a decrease of biotinylated membrane β_1-integrin in PAI-1/uPAR complex-treated podocytes. Such changes were not observed in podocytes treated with uPA, PAI-1 alone, or the anti-uPAR + PAI-1/uPA complex. *B*: β_1-integrin was increased in the cytoplasmic fraction in PAI-1/uPAR-treated podocytes. *C*: double immunogold labeling by immunoelectron microscopy of β_1-integrin (5-nm gold particles) and uPAR (10-nm gold particles). For uPA, both β_1-integrin and uPAR were predominantly located on the cell surface, whereas PAI-1/uPA showed colocalization of both proteins in the cytoplasm. Note that gold particles of both sizes were associated with endocytotic vesicles (*inset*). Scale bars = 50 nm. *D*: under ×40,000 magnification, gold particles of both sizes were counted, and the particle ratio in the cell membrane and total numbers of particles were calculated. Ratios of β_1-integrin and uPAR were significantly reduced in podocytes treated with PAI-1/uPA (n = 6) than in those treated with uPA (n = 4). *$P < 0.05$.

findings shed light into the new therapeutic strategies targeting podocyte integrin signaling.

In conclusion, primary podocyte injury stimulates upregulation of endothelial PAI-1, with the uPA/uPAR complex on the podocyte surface, resulting in podocyte detachment secondary to β_1-integrin endocytosis (Fig. 10). This mechanism may explain a vicious cycle of podocyte injury. Therefore, we suggest PAI-1 inhibition as a possible therapeutic option for the progression of glomerular injury inhibiting the vicious podocyte domino effect.

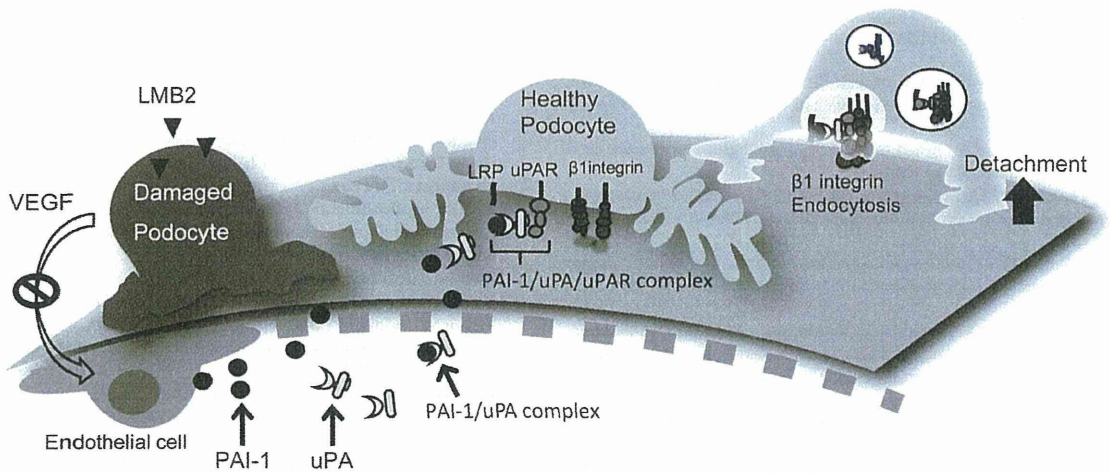

Fig. 10. Schematic demonstration of the podocyte domino effect by PAI-1/uPAR-mediated β_1-integrin endocytosis. From the *left*, damaged podocytes repressed VEGF expression, leading to endothelial dysfunction. Damaged endothelial cells produced and secreted PAI-1 (molecular mass: 45 kDa), which binds to circulating uPA (molecular mass: 31.5 kDa) either in the capillary or on the podocyte surface and then makes a complex with uPAR on the podocyte surface. The complex formation is able to bind β_1-integrin, which is known as a strong assembler of podocyte-GBM attachment. With the aid of a large endocytotic receptor, LDL receptor-related protein (LRP), on the podocyte surface (the expression of LRP was detected in vivo and cultured podocytes by real-time PCR in our preliminary experiments), β_1-integrin is translocated to the podocyte cytoplasm by endocytosis with the PAI-1/uPA/uPAR complex. Finally, β_1-integrin-lost primary healthy podocytes undergo detachment from the GBM.

ACKNOWLEDGMENTS

The authors thank Dr. Toru Sakairi for providing the mouse podocyte cell line.

GRANTS

This work was supported in part by the Intramural Research Program of the National Institutes of Health, National Cancer Institute, Center for Cancer Research, Grants-In-Aid for Scientific Research from the Japan Society for the Promotion of Science (KAKEN; Research Project nos. 22590877 and 26461210), Progressive Renal Disease Research of the Ministry of Health, Labor and Welfare of Japan, and Astellas Pharma in Japan.

DISCLOSURES

J. Reiser is the inventor of patents that aim to develop novel assays and drugs for proteinuric kidney diseases. He stands to gain royalties from their commercialization.

AUTHOR CONTRIBUTIONS

Author contributions: N.K., T.U., K.O., H.Y., Y. Takahashi, K.S., S.M., S.H., Y. Takashima, T.D., I.P., H.K., and T. Matsusaka performed experiments; N.K., T.U., Y. Takahashi, and M.N. analyzed data; N.K., T.U., J.R., and M.N. interpreted results of experiments; N.K. and Y. Takahashi prepared figures; N.K. and M.N. drafted manuscript; Y. Takahashi and M.N. approved final version of manuscript; T.D., I.P., T. Miyata, T. Matsusaka, and M.N. conception and design of research.

REFERENCES

1. **Aita K, Etoh M, Hamada Yokoyama C H, Takahashi A, Suzuki T, Hara M, Nagata M.** Acute and transient podocyte loss and proteinuria in preeclampsia. *Nephron Clin Pract* 112: c65–c70, 2009.
2. **Bergstein JM, Riley M, Bang NU.** Role of plasminogen-activator inhibitor type 1 in the pathogenesis and outcome of the hemolytic uremic syndrome. *N Engl J Med* 327: 755–759, 1992.
3. **Bolte S, Cordelières FP.** A guided tour into subcellular colocalization analysis in light microscopy. *J Microsc* 224: 213–232, 2006.
4. **Brooks PC, Klemke RL, Schon S, Lewis JM, Schwartz MA, Cheresh DA.** Insulin-like growth factor receptor cooperates with integrin alpha v beta 5 to promote tumor cell dissemination in vivo. *J Clin Invest* 99: 1390–1398, 1997.
5. **Czekay RP, Aertgeerts K, Curriden SA, Loskutoff DJ.** Plasminogen activator inhibitor-1 detaches cells from extracellular matrices by inactivating integrins. *J Cell Biol* 160: 781–791, 2003.
6. **Czekay RP, Loskutoff DJ.** Plasminogen activator inhibitors regulate cell adhesion through a uPAR-dependent mechanism. *J Cell Physiol* 220: 655–663, 2009.
7. **D'Agati VD.** Podocyte injury in focal segmental glomerulosclerosis: lessons from animal models (a play in five acts). *Kidney Int* 73: 399–406, 2008.
8. **D'Agati VD, Kaskel FJ, Falk RJ.** Focal segmental glomerulosclerosis. *N Engl J Med* 365: 2398–2411, 2011.
9. **Dellas C, Loskutoff DJ.** Historical analysis of PAI-1 from its discovery to its potential role in cell motility and disease. *Thromb Haemost* 93: 631–640, 2005.
10. **Eddy AA, Fogo AB.** Plasminogen activator inhibitor-1 in chronic kidney disease: evidence and mechanisms of action. *J Am Soc Nephrol* 17: 2999–3012, 2006.
11. **Elzi DJ, Lai Y, Song M, Hakala K, Weintraub ST, Shiio Y.** Plasminogen activator inhibitor 1-insulin-like growth factor binding protein 3 cascade regulates stress-induced senescence. *Proc Natl Acad Sci USA* 109: 12052–12057, 2012.
12. **Eremina V, Jefferson JA, Kowalewska J, Hochster H, Haas M, Weisstuch J, Richardson C, Kopp JB, Kabir MG, Backx PH, Gerber HP, Ferrara N, Barisoni L, Alpers CE, Quaggin SE.** VEGF inhibition and renal thrombotic microangiopathy. *N Engl J Med* 358: 1129–1136, 2008.
13. **George M, Rainey MA, Naramura M, Foster KW, Holzapfel MS, Willoughby LL, Ying G, Goswami RM, Gurumurthy CB, Band V, Satchell SC, Band H.** Renal thrombotic microangiopathy in mice with combined deletion of endocytic recycling regulators EHD3 and EHD4. *PLos One* 6: e17838, 2011.
14. **Hamano K, Iwano M, Akai Y, Sato H, Kubo A, Nishitani Y, Uyama H, Yoshida Y, Miyazaki M, Shiiki H, Kohno S, Dohi K.** Expression of glomerular plasminogen activator inhibitor type I in glomerulonephritis. *Am J Kidney Dis* 39: 695–705, 2002.
15. **Hayashida T, Jones JC, Lee CK, Schnaper HW.** Loss of β1-integrin enhances TGF-β1-induced collagen expression in epithelial cells via increased αvβ3-integrin and Rac1 activity. *J Biol Chem* 285: 30741–30751, 2010.
16. **Hedberg A, Fismen S, Fenton KA, Fenton C, Osterud B, Mortensen ES, Rekvig OP.** Heparin exerts a dual effect on murine lupus nephritis by enhancing enzymatic chromatin degradation and preventing chromatin binding in glomerular membranes. *Arthritis Rheum* 63: 1065–1075, 2011.
17. **Ichimura A, Matsumoto S, Suzuki S, Dan T, Yamaki S, Sato Y, Kiyomoto H, Ishii N, Okada K, Matsuo O, Hou FF, Vaughan DE, van Ypersele de Strihou C, Miyata T.** A small molecule inhibitor to plasminogen activator inhibitor 1 inhibits macrophage migration. *Arterioscler Thromb Vasc Biol* 33: 935–942, 2013.
18. **Izuhara Y, Takahashi S, Nangaku M, Takizawa S, Ishida H, Kurokawa K, van Ypersele de Strihou C, Hirayama N, Miyata T.** Inhibition of plasminogen activator inhibitor-1: its mechanism and effectiveness on coagulation and fibrosis. *Arterioscler Thromb Vasc Biol* 28: 672–677, 2008.
19. **Izuhara Y, Yamaoka N, Kodama H, Dan T, Takizawa S, Hirayama N, Meguro K, van Ypersele de Strihou C, Miyata T.** A novel inhibitor of plasminogen activator inhibitor-1 provides antithrombotic benefits devoid of bleeding effect in nonhuman primates. *J Cereb Blood Flow Metab* 30: 904–912, 2010.
20. **Kitching AR, Kong YZ, Huang XR, Davenport P, Edgtton KL, Carmeliet P, Holdsworth SR, Tipping PG.** Plasminogen activator inhibitor-1 is a significant determinant of renal injury in experimental crescentic glomerulonephritis. *J Am Soc Nephrol* 14: 1487–1495, 2003.
21. **Kriz W, Gretz N, Lemley KV.** Progression of glomerular diseases: is the podocyte the culprit? *Kidney Int* 54: 687–697, 1998.
22. **Kriz W, Shirato I, Nagata M, LeHir M, Lemley KV.** The podocyte's response to stress: the enigma of foot process effacement. *Am J Physiol Renal Physiol* 304: F333–F347, 2013.
23. **Kurihara H, Harita Y, Ichimura K, Hattori S, Sakai T.** SIRP-α-CD47 system functions as an intercellular signal in the renal glomerulus. *Am J Physiol Renal Physiol* 299: F517–F527, 2010.
24. **Lijnen HR.** Pleiotropic functions of plasminogen activator inhibitor-1. *J Thromb Haemost* 3: 35–45, 2005.
25. **Matsusaka T, Sandgren E, Shintani A, Kon V, Pastan I, Fogo AB, Ichikawa I.** Podocyte injury damages other podocytes. Podocyte injury damages other podocytes. *J Am Soc Nephrol* 22: 1275–1285, 2011.
26. **Matsusaka T, Xin J, Niwa S, Kobayashi K, Akatsuka A, Hashizume H, Wang QC, Pastan I, Fogo AB, Ichikawa I.** Genetic engineering of glomerular sclerosis in the mouse via control of onset and severity of podocyte-specific injury. *J Am Soc Nephrol* 16: 1013–1023, 2005.
27. **Nagata M, Kriz W.** Glomerular damage after uninephrectomy in young rats. II. Mechanical stress on podocytes as a pathway to sclerosis. *Kidney Int* 42: 148–160, 1992.
28. **Nagata M.** Pathogenesis of glomerulosclerosis: role of epithelial interactions. *Clin Exp Nephrol* 4: 173–181, 2000.
29. **Nakamura T, Tanaka N, Hoguma N, Kazama T, Kobayashi I, Yokota S.** The localization of plasminogen activator inhibitor-1 in glomerular subepithelial deposits in membranous nephropathy. *J Am Soc Nephrol* 11: 2434–2444, 1996.
30. **Pozzi A, Jarad G, Moeckel GW, Coffa S, Zhang X, Gewin L, Eremina V, Hudson BG, Borza DB, Harris RC, Holzman LB, Phillips CL, Fassler R, Quaggin SE, Miner JH, Zent R.** β1 integrin expression by podocytes is required to maintain glomerular structural integrity. *Dev Biol* 316: 288–301, 2008.
31. **Rau JC, Beaulieu LM, Huntington JA, Church FC.** Serpins in thrombosis, hemostasis and fibrinolysis. *J Thromb Haemost* 5: 102–115, 2007.
32. **Sachs N, Sonnenberg A.** Cell-matrix adhesion of podocytes in physiology and disease. *Nat Rev Nephrol* 9: 200–210, 2013.
33. **Sakairi T, Abe Y, Jat PS, Kopp JB.** Cell-cell contact regulates gene expression in CDK4-transformed mouse podocytes. *Am J Physiol Renal Physiol* 299: F802–F809, 2010.
34. **Schneider CA, Rasband WS, Eliceiri KW.** NIH Image to ImageJ: 25 years of image analysis. *Nat Methods* 9: 671–675, 2012.
35. **Schneider DJ, Chen Y, Sobel BE.** The effect of plasminogen activator inhibitor type 1 on apoptosis. *Thromb Haemost* 100: 1037–1040, 2008.

36. **Slater SC, Ramnath RD, Uttridge K, Saleem MA, Cahill PA, Mathieson PW, Welsh GI, Satchell SC.** Chronic exposure to laminar shear stress induces Kruppel-like factor 2 in glomerular endothelial cells and modulates interactions with co-cultured podocytes. *Int J Biochem Cell Biol* 44: 1482–1490, 2012.
37. **Smith HW, Marshall CJ.** Regulation of cell signalling by uPAR. *Nat Rev Mol Cell Biol* 11: 23–36, 2010.
38. **Takemoto M, Asker N, Gerhardt H, Lundkvist A, Johansson BR, Saito Y, Betsholtz C.** A new method for large scale isolation of kidney glomeruli from mice. *Am J Pathol* 161: 799–805, 2002.
39. **Ueno T, Kobayashi N, Nakayama M, Takashima Y, Ohse T, Pastan I, Pippin JW, Shankland SJ, Uesugi N, Matsusaka T, Nagata M.** Aberrant Notch1-dependent effects on glomerular parietal epithelial cells promotes collapsing focal segmental glomerulosclerosis with progressive podocyte loss. *Kidney Int* 83: 1065–1075, 2013.
40. **Webb DJ, Thomas KS, Gonias SL.** Plasminogen activator inhibitor 1 functions as a urokinase response modifier at the level of cell signalling and thereby promotes MCF-7 cell growth. *J Cell Biol* 152: 741–752, 2001.
41. **Wei C, Möller CC, Altintas MM, Li J, Schwarz K, Zacchigna S, Xie L, Henger A, Schmid H, Rastaldi MP, Cowan P, Kretzler M, Parrilla R, Bendayan M, Gupta V, Nikolic B, Kalluri R, Carmeliet P, Mundel P, Reiser J.** Modification of kidney barrier function by the urokinase receptor. *Nat Med* 17: 55–63, 2008.
42. **Wei C, El Hindi S, Li J, Fornoni A, Goes N, Sageshima J, Maiguel D, Karumanchi SA, Yap HK, Saleem M, Zhang Q, Nikolic B, Chaudhuri A, Daftarian P, Salido E, Torres A, Salifu M, Sarwal MM, Schaefer F, Morath C, Schwenger V, Zeier M, Gupta V, Roth D, Rastaldi MP, Burke G, Ruiz P, Reiser J.** Circulating urokinase receptor as a cause of focal segmental glomerulosclerosis. *Nat Med* 17: 952–960, 2011.
43. **Wharram BL, Goyal M, Wiggins JE, Sanden SK, Hussain S, Filipiak WE, Saunders TL, Dysko RC, Kohno K, Holzman LB, Wiggins RC.** Podocyte depletion causes glomerulosclerosis: diphtheria toxin-induced podocyte depletion in rats expressing human diphtheria toxin receptor transgene. *J Am Soc Nephrol* 16: 2941–2952, 2005.
44. **Xu Y, Hagege J, Mougenot B, Sraer JD, Rønne E, Rondeau E.** Different expression of the plasminogen activation system in renal thrombotic microangiopathy and the normal human kidney. *Kidney Int* 50: 2011–2019, 1996.
45. **Yoshida Y, Shiiki H, Iwano M, Uyama H, Hamano K, Nishino T, Dohi K.** Enhanced expression of plasminogen activator inhibitor 1 in patients with nephrotic syndrome. *Nephron* 88: 24–29, 2001.
46. **Yu CC, Fornoni A, Weins A, Hakroush S, Maiguel D, Sageshima J, Chen L, Ciancio G, Faridi MH, Behr D, Campbell KN, Chang JM, Chen HC, Oh J, Faul C, Arnaout MA, Fiorina P, Gupta V, Greka A, Burke 3rd GW, Mundel P.** Abatacept in B7-1-positive proteinuric kidney disease. *N Engl J Med* 369: 2416–2423, 2013.

PLOS | ONE

RESEARCH ARTICLE

Nitric Oxide Prevents Alveolar Senescence and Emphysema in a Mouse Model

Amanda E. Boe[1,2], Mesut Eren[1], Luisa Morales-Nebreda[1], Sheila B. Murphy[1,2], G. R. Scott Budinger[1], Gökhan M. Mutlu[3], Toshio Miyata[4], Douglas E. Vaughan[1,2]*

1 Department of Medicine, Northwestern University Feinberg School of Medicine, Chicago, IL, United States of America, **2** Feinberg Cardiovascular Research Institute, Northwestern University Feinberg School of Medicine, Chicago, IL, United States of America, **3** Pulmonary and Critical Care Section, Department of Medicine, University of Chicago, Chicago, IL, United States of America, **4** United Centers for Advanced Research and Translational Medicine (ART), Tohoku University Graduate School of Medicine, Miyagi, Japan

* d-vaughan@northwestern.edu

OPEN ACCESS

Citation: Boe AE, Eren M, Morales-Nebreda L, Murphy SB, Budinger GRS, Mutlu GM, et al. (2015) Nitric Oxide Prevents Alveolar Senescence and Emphysema in a Mouse Model. PLoS ONE 10(3): e0116504. doi:10.1371/journal.pone.0116504

Academic Editor: Rory Edward Morty, University of Giessen Lung Center, GERMANY

Received: October 24, 2014

Accepted: December 1, 2014

Published: March 10, 2015

Data Availability Statement: All relevant data are within the paper.

Funding: This work was funded by grants 1P01HL108795-01 and R01HL051387, both awarded to DEV by the National Institutes of Health (www.nih.gov). This work was also supported by Northwestern University's Center for Advanced Microscopy and a Cancer Center Support Grant (NCI CA060553). The funders had no role in study design, data collection and analysis, decision to publish, or preparation of the manuscript.

Abstract

N^{ω}-nitro-L-arginine methyl ester (L-NAME) treatment induces arteriosclerosis and vascular senescence. Here, we report that the systemic inhibition of nitric oxide (NO) production by L-NAME causes pulmonary emphysema. L-NAME-treated lungs exhibited both the structural (alveolar tissue destruction) and functional (increased compliance and reduced elastance) characteristics of emphysema development. Furthermore, we found that L-NAME-induced emphysema could be attenuated through both genetic deficiency and pharmacological inhibition of plasminogen activator inhibitor-1 (PAI-1). Because PAI-1 is an important contributor to the development of senescence both *in vitro* and *in vivo*, we investigated whether L-NAME-induced senescence led to the observed emphysematous changes. We found that L-NAME treatment was associated with molecular and cellular evidence of premature senescence in mice, and that PAI-1 inhibition attenuated these increases. These findings indicate that NO serves to protect and defend lung tissue from physiological aging.

Introduction

We have previously reported that chronic exposure to the nitric oxide synthase (NOS) inhibitor N^{ω}-nitro-L-arginine methyl ester (L-NAME) causes hypertension, arteriosclerosis, and vascular senescence in mice [1,2,3]. The development of these pathologies can be attenuated through either genetic deficiency [1,2] or pharmacologic inhibition [3] of plasminogen activator inhibitor-1 (PAI-1). These studies defined the *in vivo* roles of both nitric oxide (NO) and PAI-1 in vascular senescence. While the vascular biology of NO often focuses on its vasodilator properties, NO can also alter proteins through posttranslational modification via S-nitrosylation to form S-nitrosothiols (SNOs). SNO-based signaling plays a major role in oxygen sensing, delivery, and utilization, and SNO-modified proteins affect the respiratory cycle, pulmonary gas exchange, and ventilation [4]. Therefore, we sought to expand upon our previous work and determine what role, if any, NO and PAI-1 has in lung tissue.

Competing Interests: The authors have declared that no competing interests exist.

Materials and Methods

Experimental animals and L-NAME/TM5441 administration

Studies were performed on littermate 6–8 week old C57BL/6J mice (either WT or PAI-$1^{-/-}$) of both sexes purchased from Jackson Laboratories (Bar Harbor, ME). L-NAME (Sigma Aldrich, St. Louis, MO) was administered in the drinking water at 1 mg/mL (approximately 100–120 mg/kg/day). TM5441 was mixed in the chow at a concentration of 20 mg/kg/day as described previously [3]. Mice remained in the study for either 1 week or 8 weeks before undergoing final measurements and tissue harvest.

Ethics Statement

All work was performed as proposed in experimental Animal Study Protocol 2012–1771, which was approved by the Institutional Animal Care and Use Committee of Northwestern University. Euthanasia was carried out with Isoflurane followed by cervical dislocation for tissue harvest. Every effort was made to minimize suffering.

qRT-PCR

Lungs harvested from mice were snap frozen in liquid nitrogen. 15–40 mg of tissue was weighed out for RNA isolation using the Qiagen RNeasy Mini Kit (Qiagen, Valencia, CA) by following the manufacturer's protocol. cDNA was generated from the RNA using the qScript cDNA Supermix (Quanta Biosciences, Gaithersburg, MD) by following the manufacturer's protocol. cDNA concentration was quantified using the Take 3 software and plate reader (Bio-Tek Instruments, Winooski, VT). Samples were then diluted to generate 0.1μg/μL solutions.

Quantitative real-time PCR (qRT-PCR) was performed using the SsoAdvanced SYBR Green Supermix (Biorad, Hercules, CA) with primers for $p16^{Ink4a}$ (F: 5'-AGGGCCGTGTGCATGACGTG-3' and R: 5'-GCACCGGGCGGGAGAAGGTA-3'), p53 (F: 5'-GGCCCAAGTGAAGCCCTCCG-3' and R: 5'-GCCCAGGGGTCTCGGTGACA-3'), p21 (F: 5'-GGACGTCCCACTTTGCCAGCAG-3' and R: 5'-GAGCGCATCGCAATCACGGC-3'), and GAPDH (F: 5'-ATGTTCCAGTATGACTCCACTCACG-3' and R: 5'-GAAGACACCAGTAGACTCCACGACA-3') (Integrated DNA Technologies, Inc., Coralville, IA). Primers were resuspended at 100 μM and then diluted to generate 10 μM solutions. Reaction set up was as follows: 4.6 μL cDNA, 10 μL SYBR Supermix, 1 μL of both forward and reverse primers, 3.4 μL nuclease free water. Cycling conditions were: 95°C for 30 seconds, 40 cycles of 95°C for 5 seconds and 59°C for 15 seconds (CFX Connect Real-Time System, BioRad, Hercules, CA).

Average telomere length ratio

Lungs harvested from mice were snap frozen in liquid nitrogen. Genomic DNA was isolated from 15–40 mg of lung tissue using the Qiagen DNeasy Blood & Tissue Kit (Qiagen, Valencia, CA) by following the manufacturer's protocol. Telomere length was measured using quantitative real-time PCR as previously described with minor modification [5,6]. Briefly, telomere repeats are amplified using specially designed primers. These are then compared to the amplification of a single-copy gene, the 36B4 gene (acidic ribosomal phosphoprotein PO), to determine the average telomere length ratio (ATLR). Either 15 ng (aortas), 100 ng (livers), or 20 ng (lungs) of genomic DNA template was added to each 20 μl reaction containing forward and reverse primers (250 nM each for telomere primers, and 500 nM each for the 36B4 primers), SsoAdvanced SYBR Green Supermix (Biorad, Hercules, CA), and nuclease free water. A serially diluted standard curve of 25 ng to 1.5625 ng (aortas), 100 ng to 3.125 ng (livers), or 50 to 1.5625 (lungs) per well of template DNA from a WT mouse sample was included on each plate for both the telomere